Chapter 3

A Hydrous Manganese Oxide Doped Gel Probe Sampler for Measuring *In Situ* Reductive Dissolution Rates: I. Laboratory Development

Abstract

Reductive dissolution of redox-sensitive minerals such as manganese (Mn) oxides in natural sediments is an important mechanism for trace element mobilization into groundwater. A gel probe sampler has been constructed to study *in situ* reductive dissolution of Mn oxides. The gel consists of a polyacrylamide polymer matrix doped with hydrous Mn oxide (HMO). Gel slabs are mounted into a probe, which is designed to be inserted into the sediments. The amount of Mn released from the gel by reductive dissolution is determined by comparing the amount of Mn initially embedded into the gel with the amount remaining in the gel after exposure to conditions in the sediments or, in laboratory studies, to reducing agents. In this laboratory study, the performance of the gel probes was examined using the model reductant ascorbate and the Mn-reducing bacteria *Shewanella oneidensis* strain MR-1. In addition, a 1-D model was used to relate the reaction rates observed for HMO embedded in gels to those for HMO in suspension. One limitation of the HMO-doped gels for assessing microbial reduction rates is that the

gels prevent direct contact between the microbes and the HMO and hence preclude enzymatic reduction at the cell surface. Nonetheless, the HMO-doped gel probes offer the possibility to establish a lower bound for Mn-reduction capacity in sediments.

Introduction

Manganese (Mn) is an important and abundant element in the aqueous environment. Mn oxide solids are well-known sinks for metals and metalloids via sorption, and microbially mediated reduction of Mn oxides has been linked to the release of metals and metalloids to porewater (Lovley 1991). Biogeochemical cycling of Mn thus has implications for the cycling of other trace elements that pose a hazard to human health.

Furthermore, Mn(III,IV) oxide formation and reductive dissolution are key processes in the redox cycling of Mn and other redox-sensitive elements in sediments. The distribution of these elements with depth in sediment porewaters reflects the intensity of chemical and biological redox reactions during early diagenesis, such as the diffusion of dissolved chemical species and the rate of sediment accumulation (Berner 1980). Microbial processes dominate Mn(II) oxidation in the environment, as biological Mn oxidation is generally fast relative to abiotic Mn oxidation processes, including surface-catalyzed reactions (Davies and Morgan 1989, Morgan 2000). On the other hand, Mn(III,IV) oxides are readily reduced by both chemicals (Stone and Morgan 1984, Burdige and Nealson 1986, de Vitre et al. 1988, Wang and Stone 2006b, 2006a) and microbes (Myers and Nealson 1988a, Burdige et al. 1992, Ruebush et al. 2006). Porewater geochemistry can be assessed through a variety of methods, but the method of diffusive equilibrium in thin films (DET) has proven to be amenable to modifications for the assessment of processes occurring in sediments (Edenborn et al. 2002, Campbell et al.

2008a). The DET method uses polyacrylamide gels placed in a plastic holder, covered with a permeable membrane, and inserted vertically into sediments. The water inside the gel is allowed to equilibrate with the surrounding porewater solution via diffusion, and the composition of the ambient porewater can be determined upon removal. The early model of this device by Davison et al. (1994) used a single polyacrylamide gel slab; a modified ladder structure has been used more recently (Fones et al. 1998, Kneebone et al. 2002, Campbell et al. 2008b).

Polyacrylamide gels doped with Fe oxides have been used to evaluate of the effect of porewater composition on *in situ* sorption (Campbell et al. 2008a, 2008b). Similar probes containing agarose gels doped with Mn oxides have been used as qualitative redox indicators (Edenborn et al. 2002). These Mn oxide-doped gels take advantage of the high redox potential for Mn oxide reduction, as well as the pronounced difference in the solubility of largely insoluble Mn(III,IV) oxides as compared with the relatively soluble Mn(II) containing solids (Morgan 2000). Thus, under reducing conditions, Mn(II) can diffuse out of gels.

The purpose of this study was to develop and validate a method to quantify *in situ* rates of reductive dissolution as a function of depth along a sediment profile by using a hydrous Mn oxide (HMO) doped gel probe sampler. Reductive dissolution of HMO is quantified by measuring Mn mass loss over the course of deployment in sediments. Laboratory validation of this method was performed using two model systems—one abiotic and one biotic. Ascorbate was used for abiotic experiments since it is an analog for some functional groups found in natural organic matter (Stone and Morgan 1984). *Shewanella oneidensis* MR-1, used in the biotic experiments, is a facultative anaerobe

with a highly versatile electron transport chain (Ruebush et al. 2006) and a single polar flagellum (Abboud et al. 2005).

Experimental Section

Reagents

All chemicals used were reagent grade (Omnipure, EM Science unless otherwise noted) and used without further purification. All water used was 18 MΩ-cm deionized water (Elix/Milli-Q, Millipore). Solutions were stored in plastic containers that had been acid-washed in 5% hydrochloric acid. All nitric acid solutions were made with trace metal grade HNO_3 (70%). All hydroxylamine solutions were made with trace metal grade hydroxylamine.

HMO synthesis

The HMO precipitate was prepared by adding 50 ml of 0.02 M $KMnO_4$ (adjusted to pH 12.5 with 1M NaOH) dropwise to a stirred solution of 100 ml of 0.03 M $MnSO_4 \cdot H_2O$ (adjusted to pH 7 with 1M NaOH), following the method of Murray (1974). The stirred suspension was allowed to equilibrate over 4 h while the pH stabilized. After 4 h, the HMO was washed 3 times with water, and the precipitate was resuspended in 200 ml of water, with a resulting concentration of approximately 40 mM Mn (3.5 g l^{-1}). This form of HMO is an abiotic analog of biogenic Mn oxide best termed "triclinic Na-birnessite" (Villalobos et al. 2003, Jurgensen et al. 2004).

X-ray diffraction (Phillips X'Pert PRO, Cu-Kα X-ray source) analysis confirmed that the HMO was largely amorphous, with slightly increasing crystallinity over two

weeks. HMO was used within two weeks of synthesis to decrease the impact of changing crystallinity over time. The specific surface area measured by BET-N_2 surface adsorption was 60 m^2 g^{-1}, which declined to 38 m^2 g^{-1} after 3 weeks, consistent with that of similar amorphous Mn oxide solids (Villalobos et al. 2003, Kennedy et al. 2004). Finally, the average oxidation state of the HMO solid, measured via a modified Winkler titration (Carpenter 1965), was 3.7 ± 0.1, again consistent with the values (3.6–4.0) for similar amorphous Mn oxide solids (Villalobos et al. 2003, Jurgensen et al. 2004).

Gels and gel probes

Polyacrylamide gel slabs were made by modifying the methods of Davison et al. (1994), Kneebone et al. (2002), and Campbell et al. (2008a). Gels were made by dissolving 3.75 g acrylamide (C_3H_5NO) and 0.075 g N-N'-methylene-bis-acrylamide ($(CH_2CHCONH)_2CH_2$) in either 25 ml of water (clear gels) or 7.5 ml HMO stock diluted with 17.5 ml water (HMO-doped gels). The resulting solution was deoxygenated by bubbling with compressed argon for 30–45 minutes. The simultaneous addition of 150 µl of 100g l^{-1} sodium persulfate and 25 µl of tetramethylethylenediamine (TEMED) initiated the polymerization of the gel. The solution was mixed and quickly poured into a heated, acid-washed, glass Petri dish to increase the polymerization rate. Over 4 minutes, the gel completely solidified, upon which the dish was removed from the heat. After the gel cooled to room temperature, it was gently extracted from the Petri dish with a flexible plastic spatula and transferred directly into 1 l water, in which it hydrated for approximately 24 h.

Gel slabs were hand-cut with a plastic, acid-washed blade into the appropriate size (5 mm × 25 mm, 2 mm thick) for a ladder-style gel probe and stored in water for up

to one week to prevent dehydration. Gel probes were designed to hold the gel slabs in slots etched into a plastic holder, as described in previous work (Campbell et al. 2008b). "Mini-probes" were 4 cm long with a single column of six slots for gel slabs.

Ten gels from each batch of gel slabs were each placed in 10 ml of 0.5% hydroxylamine-HCl for ≥ 12 h to dissolve the HMO out of each gel. The supernatant was diluted and analyzed with ICP-MS to determine the total Mn in the gel, which averaged 1.50 μmol per gel, with less than 15% variation between batches of gels (some gels were excluded due to visual heterogeneity in Mn oxide distribution). Similarly, once a gel slab had reacted with a solution, the gel slab was removed and equilibrated for ≥ 12 h with 0.5% hydroxylamine-HCl, which reductively dissolved any remaining HMO solid. The equilibrating solution was diluted with 1% HNO_3 and analyzed for total dissolved Mn via ICP-MS.

Laboratory experiments

A series of laboratory-based experiments were conducted to determine the abiotic and microbially mediated rates of HMO reductive dissolution in suspension and in doped polyacrylamide gels. All laboratory experiments were conducted in triplicate.

Abiotic reduction

HMO (diluted from the 3.5 g l^{-1} stock suspension), HMO-doped gels, or HMO-doped mini-probes were added to solutions of 2 mM L-ascorbic acid (Sigma) and in 33 mM Na_2SO_4 (Fisher; I = 0.1 M) buffered to pH 8.0 with 2 mM HEPES buffer. As needed, pH was adjusted by addition of 0.1 M NaOH or H_2SO_4. The total HMO concentration in all non-mini-probe experiments was approximately 4–6 times that of the mini-probe

experiments. Over 6 h, samples were taken from the stirred bulk solution, syringe-filtered (Whatman 0.2 μm mixed cellulose ester filters), and acidified in 1% HNO_3 for analysis via ICP-MS. Because of the slow rate of Mn(II) oxidation by O_2 (Morgan 2005), the total Mn remaining in recovered gel slabs at the end of the experiments was measured to confirm the mass balance. The bulk solution, gel storage bath, and recovered gels accounted for over 95% of the total Mn (Table A.1).

Microbially mediated reduction

Experiments with *S. oneidensis* MR-1 were conducted anaerobically, either in sealed anaerobic culture bottles (HMO and HMO-doped gels) or under N_2 in a glovebox (HMO-doped mini-probes). Inocula for anaerobic cultures were grown aerobically (overnight at 30°C) in Luria Broth to stationary phase (~ 10^{12} cells l^{-1}). Cells were transferred without washing to MR-1 minimal medium (pH 8; Table A.2), containing 6 mM lactate and amended with HMO, to achieve a cell density of ~ 10^{11} cells l^{-1}. The medium contained a small amount of Mn(II), which was taken into account in subsequent Mn measurements. Culture bottles were sealed with rubber stoppers and aluminum caps and shaken at 30°C. An observed turbidity increase, indicating microbial growth over the course of the experiments, was not quantified. Samples were removed through the rubber stoppers via N_2-flushed syringes, over 8 h for HMO and over 36 h for HMO-doped gels. HMO-doped mini-probes were deployed in stirred plastic beakers at room temperature (22°C) in a glovebox. Over 63 h, these samples were removed from the bulk solution in N_2-flushed syringes. All samples were subsequently filtered and acidified as in the abiotic experiments.

Data analysis

The stoichiometry of abiotic reduction at pH 8 is shown in equation (3-1).

$$MnO_2 + C_6H_7O_6^- \rightarrow Mn(II) + C_6H_5O_6^- + 2\ OH^- \quad (3\text{-}1)$$

The rate of reductive dissolution is assumed to be equal to the rate of Mn(II) production, with a rate expression shown in equation (3-2), where the rate coefficient for the reduction of the solid MnO_2 was calculated by measuring the increase in the concentration of Mn(II) in solution as a function of time, and solving the rate expression. This expression assumes that the second e^- transfer from Mn(III) to Mn(II) is instantaneous (Stone and Morgan 1987), and that the reactivity of ascorbic acid intermediates does not affect the 1:1 stoichiometry between Mn(IV) and $C_6H_7O_6^-$ (Toner and Sposito 2005).

$$\frac{d[Mn(II)]}{dt} = k\,[C_6H_7O_6^-]_t\,[MnO_2]_t \quad (3\text{-}2)$$

Here $[MnO_2]$ represents the moles of Mn solid per volume, giving k units of $M^{-1}\ s^{-1}$. Multiplying k by the Mn oxide surface loading ($m^2\ l^{-1}$) yields the surface-area-normalized rate coefficient, k_{SA} ($m^2\ mol^{-1}\ s^{-1}$). As the reaction proceeds, the concentration of MnO_2, $[MnO_2]_t$, decreases and its value is assumed to be equal to the initial MnO_2 concentration, $[MnO_2]_0$, minus the dissolved Mn concentration, $[Mn(II)]_t$, at the sampling time (equation (3-3)).

$$[MnO_2]_t = [MnO_2]_0 - [Mn(II)]_t \quad (3\text{-}3)$$

Mn(III) produced in the course of Mn(IV) reduction is assumed either to remain in the crystal lattice or to adsorb to the oxide surface until further reduction in the absence of a strong complexing agent (Morgan 2000). The presence of excess ascorbate at this pH

should guarantee that the effect of reoxidation of any readsorbed Mn(II) on equation (3-3) is negligible (Toner and Sposito 2005).

The concentration of ascorbate, $[C_6H_7O_6^-]_t$, also decreases as the reaction proceeds, according to the stoichiometry of equation (3-1); however ascorbate concentrations were deliberately maintained in approximately tenfold excess of the total Mn in the system so that the ascorbate concentration could be assumed to be roughly constant. Thus, the rate of reductive dissolution can be expressed as in equation (3-4) below.

$$\frac{d[Mn(II)]}{dt} = k[C_6H_7O_6^-]_0([MnO_2]_0 - [Mn(II)]_t) = k'([MnO_2]_0 - [Mn(II)]_t) \quad (3\text{-}4)$$

Integrating this differential equation with respect to time yields the expression in equation (3-5).

$$\ln\left(\frac{[MnO_2]_0}{[MnO_2]_0 - [Mn(II)]_t}\right) = k't \quad (3\text{-}5)$$

Plots of the left-hand side of equation (3-5) vs. time have been fitted with linear regression (performed in Microsoft Excel). The slope of the regression line is equal to k′ (t^{-1}), and the y-intercept is theoretically 0. Statistical differences between apparent rate coefficients and between y-intercepts and zero were assessed with the t-test at a significance level of 95% in Microsoft Excel.

This approach was extended to describe microbially mediated reductive dissolution by making the simplifying assumption that this reaction occurs via a hypothetical reductant, Red, with a constant concentration (see also discussion below).

One-dimensional model

To separate the diffusion component from the chemical reduction component of the observed reaction rates, a one-dimensional diffusion-reaction model was applied to the experimental data using AQUASIM 2.1 (Reichert 1994). This model represented an HMO-doped gel as a "biofilm reactor compartment" (at zero growth rate) containing a solid matrix with well-mixed water in the pore space (92% porosity). The chemical reduction of HMO to Mn(II), whose kinetics were represented as equation (3-2) above, was limited to the pore space of this compartment. The stirred bulk solution was represented as a "mixed reactor compartment". The two compartments were connected with a "diffusive link", modeling a diffusive boundary layer for the dissolved Mn(II) and the reductant.

Initial conditions in the simulations were set to match the experimental conditions, normalized to one gel, as summarized in Table A.3. Initially, all of the Mn was confined to the gel pore space as HMO, and all of the reductant was confined to the mixed reactor. In the microbial experiments, the hypothetical reductant Red was substituted for ascorbate in equation (3-2); the diffusion coefficients for ascorbate were also used for Red. For the microbial experiments with HMO in suspension, direct (presumably enzymatic) reduction at the cell surface was incorporated as shown in equation (3-6):

$$\frac{d[Mn(II)]}{dt} = k''[MnO_2]_t \, . \qquad (3\text{-}6)$$

This mechanism, however, was excluded for HMO-doped gels (see Discussion). Simulations were performed in "Parameter Estimation" mode, which minimizes χ^2 values between the model and the experimental data to solve for a specific parameter. Sensitivity analysis determined the most useful fitting parameter for each experiment. The χ^2 values were converted to p-values, which indicate the probability that the modeled

system would generate the measured experimental data, with 100% (p-value of 1.00) being ideal goodness of fit.

Results

Laboratory experiments

Dissolved Mn was found to diffuse out of the gels in the absence of an externally added reductant. Prior to the reductive dissolution experiments, the HMO-doped gels were stored and, in the case of microbial studies, deoxygenated in Milli-Q water. It was observed that a substantial fraction of the total initial Mn (generally ≤ 20%) diffused out of the gels during deoxygenation and storage, which was attributable to desorption of Mn(II) sorbed to the HMO surface. Note that Mn(II) is present in stoichiometric excess in the synthesis method. In Milli-Q water, the rate of Mn loss was approximately 4.2×10^{-11} M s^{-1}. When the gels were transferred from Milli-Q water to the background electrolyte (2 mM HEPES in 33 mM Na_2SO_4) used for the abiotic experiments, however, negligible loss of Mn was observed over 5 d (data not shown).

Abiotic experiments with HMO in suspension proceeded quickly relative to experiments with HMO embedded in the gels; dissolution of the HMO in suspension was complete within 2 minutes. A lower bound of the surface-area-normalized rate coefficient based on this observation is k_{SA} = 5 m^2 $mol^{-1}s^{-1}$; the reported rate coefficient for this reaction at pH 7.2 is 4 m^2 $mol^{-1}s^{-1}$ (Stone and Morgan 1984).

Data from the other 7 experiments (Table A.5) were interpreted using the integrated form of the rate expression (equation (3-5)) as shown in Figure 3.1. The slopes, intercepts, and correlation coefficients from linear regression analysis are

summarized in Table 3.1. The slopes correspond to the apparent rate coefficients for each experiment. Insignificant differences in rate coefficients were obtained using Mn concentrations from syringe-filtered (0.2 μm) and unfiltered samples in abiotic experiments with HMO-doped gels; syringe-filtered Mn concentrations were > 90% of unfiltered Mn concentrations (data not shown). Likewise, the use of different membrane pore sizes in the mini-probe experiments did not affect the observed rates (Table 3.1). Overall, abiotic Mn release rates are 1–2 orders of magnitude faster than biotic rates, as represented by k′. Embedding HMO in gels and placing gels in mini-probes affects the observed apparent rate coefficients more in the abiotic experiments than in the biotic experiments. Microbial experiments with HMO suspension and mini-probes exhibited a lag phase (Figure 3.1b: 1 hour, and Figure 3.1c: 8 hours, respectively), which was only statistically significant for the mini-probes (Table 3.1, see Discussion).

One abiotic experiment was conducted with both clear and HMO-doped gels loaded in a single mini-probe sampler, in the expectation that the Mn concentrations in the clear gels would be the same as in the bulk solution. However, the Mn concentrations in the clear gels were three–twentyfold greater than that in the bulk solution. The co-location of the clear and HMO-doped gels in a single mini-probe appears to produce an artifact in which the dissolved Mn diffusing out of the HMO-doped gels perturbs the local environment sampled by the clear gels. This configuration should be avoided in applications.

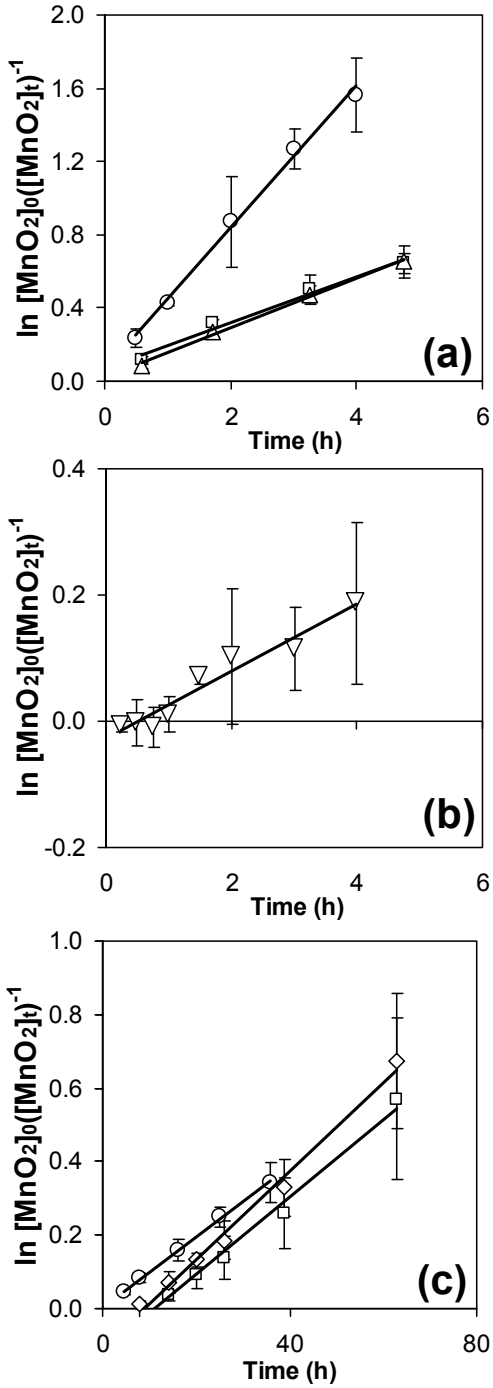

Figure 3.1. Integrated expression for the rate of Mn release, ln ($[MnO_2]_0[MnO_2]_t^{-1}$), as a function of time at pH 8.0. (a) abiotic reaction of ascorbate ($[C_6H_7O_6^-]_0$ = 2 mM) and HMO-doped gels (○; Mn_T = 184 μM) or HMO-doped gels in mini-probes with 0.45 (△; Mn_T = 52 μM) or 1.0 (□; Mn_T = 52 μM) μm membranes. (b, c) biotic reaction of *S. oneidensis* MR-1 (10^{11} cells l^{-1}) with HMO suspension (b: ▽; Mn_T = 360 μM) or (c) HMO-doped gels (○; Mn_T = 295 μM) or HMO-doped gels in mini-probes with 1.0 (□; Mn_T = 62 μM) or 5.0 (◊; Mn_T = 60 μM) μm membranes. Note difference in time axis for (c).

Table 3.1. Summary of linear regression data for laboratory-measured rates of reductive dissolution

Reductant	Oxidant	k′ (s^{-1})	±95% C.I.[a]	y-intercept	±95% C.I.	non-zero?[e]	r^2
Ascorbate	HMO[b]	5×10^{-2}	---	---	---	---	---
	HMO gels	1.0×10^{-4}	2×10^{-5}	7×10^{-2}	1×10^{-1}	no	0.99
	MP 0.45 μm[c]	3.8×10^{-5}	7×10^{-6}	2×10^{-2}	7×10^{-2}	no	1.00
	MP 1.0 μm[c]	3.5×10^{-5}	7×10^{-6}	7×10^{-2}	8×10^{-2}	yes	0.98
S. oneidensis MR-1	HMO	1.5×10^{-5}	1×10^{-5}	-3×10^{-2}	7×10^{-2}	no	0.95
	HMO gels[d]	2.7×10^{-6}	4×10^{-7}	5×10^{-3}	3×10^{-2}	no	1.00
	MP 0.45 μm[d]	2.9×10^{-6}	7×10^{-7}	-1×10^{-2}	8×10^{-2}	yes	0.99
	MP 1.0 μm[d]	3.3×10^{-6}	8×10^{-7}	-1×10^{-2}	1×10^{-1}	yes	0.99

[a] 95% confidence interval bounds for k′ (s^{-1})
[b] Rate estimated from complete dissolution in 2 minutes
[c] The rate coefficients of the two mini-probes reacted with ascorbate are not statistically different from each other.
[d] The rate coefficients of the HMO gels and the two mini-probes reduced by *S. oneidensis* MR-1 are not statistically different from each other.
[e] Is the y-intercept statistically different from zero, the initial value of ln ($[MnO_2]_0$ $[MnO_2]_t^{-1}$)?

One-dimensional model

The Mn release rates in the abiotic systems are quite different for HMO in suspension, in the gels, and in the mini-probes, even though the chemical reactants (i.e., HMO and ascorbate) are the same. This indicates that the physical properties of the systems (i.e., the embedding of the HMO in the gel and the placement of the gel in the mini-probe) must be accounted for. The AQUASIM model incorporates diffusive effects, thus allowing comparison of the different systems.

This 1-D model simulated a well-mixed bulk solution with diffusion into a gel with 92% water content, chemical reaction confined within the gel, and diffusion of the product Mn(II) into the bulk solution. Sensitivity analysis was used to identify the most useful fitting parameter for each experimental simulation: the diffusion coefficient of

ascorbate in the gel (for abiotic experiments) and the rate coefficients k″ and k′ (for the microbial experiments with HMO in suspension and in gels, respectively). Inclusion of second and third fitting parameters did not significantly improve the fit to the data.

For the two abiotic experiments, values of k derived from k′ (HMO in suspension) divided by $[C_6H_7O_6^-]_0$ (Table 3.1) were applied, and AQUASIM solved for the diffusion coefficient of ascorbate within the gel required for optimal fitting of the data (Figure 3.2). The diffusion coefficients of ascorbate in the bulk solution and Mn(II) throughout the system were adopted from literature (Yuan-Hui and Gregory 1974, Moreno et al. 2000, Nassef et al. 2007). This physical fitting parameter could account for the different Mn release rates in the two systems, so that the underlying chemical reaction rates are unaffected by the embedding of the HMO in the gel and the placement of the gel in the mini-probe.

Because the detailed mechanism in microbial reduction of metal oxides is not fully understood (Ruebush et al. 2006, O'Loughlin 2008), the AQUASIM model for microbial reduction occurred by two reactions: one with the generic reductant, Red, and the second with a surface component, k″, which required direct contact between the cells and the HMO. The surface-catalyzed reaction was therefore unavailable for HMO-doped gels and HMO-doped gels in mini-probes. For these two experiments, the model used an initial Red concentration ($[Red]_0$) fivefold greater than Mn_T for the HMO-doped gels and assigned Red the same diffusion characteristics as ascorbate in the abiotic simulations. This permitted the model to solve for k in these two experiments. AQUASIM then used the same k and $[Red]_0$ to solve for k″ in the experiment with HMO in suspension.

Chi-squared values ranged from 1.2 to 2.6 (Figure 3.2; Table A.3), which correspond with p-values greater than 0.998. Note that an 8 hour lag phase (which was not attributable to diffusion) was excluded in fitting the data from the microbial mini-probe experiment; in Figure 3.2 (right panel), time equals zero corresponds to the end of the lag period. In all cases, mass balances were satisfied for the model at steady state, with less than 1% error (Table A.4).

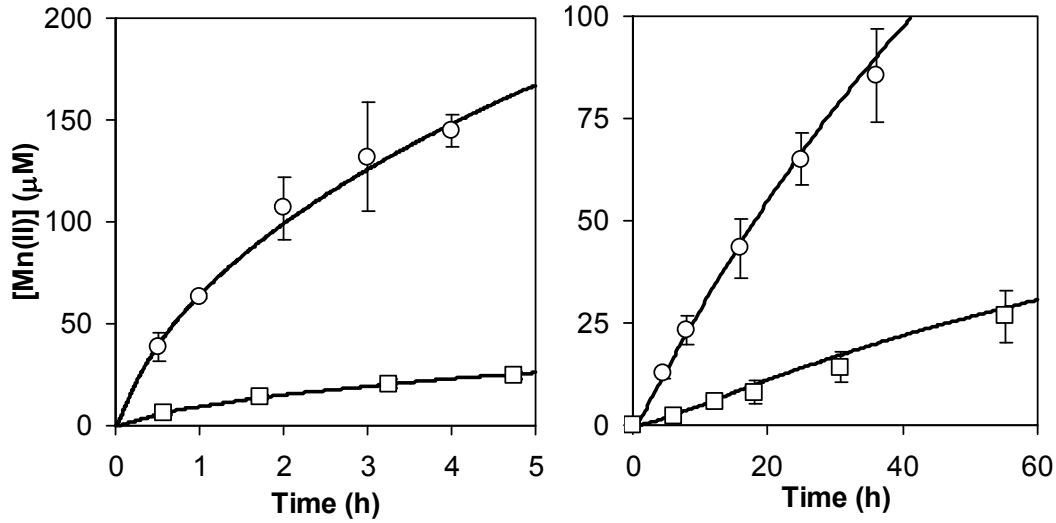

Figure 3.2. 1-D model output (lines) of Mn(II) accumulation in the bulk solution for abiotic (left) and microbially mediated (right) experiments with HMO-doped gels (○) or HMO-doped gels in mini-probes with 1.0 μm membrane (□). An 8 hour lag phase was removed from the microbial mini-probe data. Error bars are smaller than the size of the data markers in some cases. Conditions given in Figure 3.1.

Discussion

The AQUASIM modeling simulations were able to capture the physical and kinetic components of the abiotic reductive dissolution process in doped gels. The fitted value of the diffusion coefficient for ascorbate inside the gels was larger when the HMO-doped

gels were placed in the mini-probes (1.0×10^{-6} cm^2 s^{-1}) than when they were not (4.3×10^{-7} cm^2 s^{-1}). Since slower reduction was observed for HMO-doped gels in the mini-probes, this difference in the fitted diffusion coefficients can be attributed to the physical constraints of the mini-probes, which are not explicitly incorporated into the 1-D model. The bulk ascorbate diffusion coefficient is three–sevenfold larger than these gel-based diffusion coefficients, which may reflect the impact of tortuosity on diffusion in a highly porous medium (Shen and Chen 2007) or Donnan effects within the gel (Yezek and van Leeuwen 2005); both of which are presumed to be more significant for ascorbate compared to the Mn(II) ion.

The model assumed the same mechanism for microbially mediated reductive dissolution in gels: direct reduction via an external reductant (Red) diffusing into the gel. This assumption is justified because the gels and membrane prevent direct contact between *Shewanella* cells and the Mn oxide. The lack of contact is a function of dimensions: *S. oneidensis* MR-1 grown at room temperatures is approximately 0.6 μm × 3 μm in size (Abboud et al. 2005), so a membrane of pore size 0.45–5.0 μm is a strong barrier for these cells. Likewise, the largest documented pore size for polyacrylamide gels of our composition is 1.0 μm (Rüchel and Brager 1975, Chrambach 1985). Thus, cells are unlikely to enter gels, via either diffusion or chemotaxis. After 18 days of incubation, no evidence of microbial activity was found inside 3 HMO-doped gels from the sealed anaerobic culture bottles inoculated with a strain of *S. oneidensis* MR-1 that constitutively expresses a green fluorescent protein. Under a microscope (Zeiss Axioplan), the gels showed no fluorescence inside, although there was some green fluorescence at the edges of the gels (data not shown). Similarly, *Pseudomonas*

aeruginosa did not penetrate MnO_2-doped agarose gels after 1 month of incubation (Edenborn et al. 2002), so representing microbial reduction with an external reductant in the 1-D model seems appropriate.

On the other hand, the 1-D model explicitly shows that the gels do not capture all of the microbial reduction, as represented by the additional reduction mechanism required in the HMO suspension experiment. The nonzero rate coefficient k″ represents direct enzyme-catalyzed reduction at the cell surface, to which Mn oxide is inaccessible when doped in gels. In terms of the overall microbial reduction rate with HMO in suspension, k″ constitutes 65% of the total rate, whereas k′, the product of k and $[Red]_0$, constitutes the remaining 35% (Table A.3). In other words, Mn oxide-doped gels measure approximately 35% of the total reduction capacity of *S. oneidensis* MR-1.

The lower microbial reduction capacity in the gel and mini-probe model simulations could reflect either an inhibitory effect from the gel itself, or the lack of direct contact between the cells and the Mn oxide. In the former case, acrylamide is highly toxic to microorganisms (Starostina et al. 1983), and residual amounts in the polyacrylamide gels may suppress the measured reduction rates. In comparison to literature values, this study measured an HMO reduction rate of 5.4×10^{-19} mol cell^{-1} s^{-1}, which is mid-range for the values in literature (Table 3.2). Minor variations in growth medium, temperature, and Mn oxide crystallinity account for the range of over 3 orders of magnitude. The latter and more likely explanation is that prevention of direct contact between the cells and the Mn oxide in gels bypasses some portion of microbial reduction (Ruebush et al. 2006). Thus, HMO-doped gel probes only measure microbially mediated rates of reductive dissolution as generated by extracellular electron shuttles and by-

products of metabolism, rather than by direct enzymatic microbial reduction, which is a distinct artifact. These biochemical compounds are likely to be smaller than the membrane pore sizes, since like ascorbate, the pore size has no statistically significant effect on the reduction rate they produce (Table 3.1).

Table 3.2. Summary of literature values for Mn oxide reduction by *S. oneidensis* MR-1

Source	**Reported Rate (units given)**	**Growth Medium[a]**	**Mn oxide[b]**	**Rate (mol s^{-1} $cell^{-1}$)**
Burdige et al. (1992)	7.39 μM d^{-1} [c]	LO	HMO	2.14×10^{-20}
	4.65 μM d^{-1} [c]	LO	δ-MnO_2	1.35×10^{-20}
	11.8 μM d^{-1} [c]	LO	birnessite	3.43×10^{-20}
Myers and Nealson (1988a)	2.0-87×10^{-10} μmol h^{-1} $cell^{-1}$	LO	δ-MnO_2	5.6-240×10^{-20}
	1.0-4.2×10^{-8} μmol h^{-1} $cell^{-1}$	M1	δ-MnO_2	2.9-12×10^{-18}
Ruebush et al. (2006)	7.4×10^{-8} mol min^{-1} mg^{-1} [d]	M1[e]	birnessite	1.1×10^{-19}
this study	---	M1	HMO	5.4×10^{-19}

[a] LO medium is an undefined medium, whereas M1 is a defined, minimal medium.
[b] Birnessite and δ-MnO_2 are structurally similar to HMO [21].
[c] Cell number is 4×10^{6} cells ml^{-1}.
[d] Rates measured for total membrane (TM) fractions only (8.75 mg TM $cell^{-1}$)
[e] M1 medium modified with 50 mM ferric citrate (replacing fumarate), 30 mM DL-lactate, 4 mM sodium phosphate, and 10 mM HEPES

The reduction kinetics of the biochemical compounds represented by Red are much slower than the kinetics of ascorbate. The ascorbate rate coefficient is 3 orders of magnitude larger than that of Red, which is on the order of pyruvate and oxalate (Stone and Morgan 1984), but the model assumption that Red is maintained in excess of HMO is somewhat arbitrary. Instead, consider the amount of ascorbate required to generate the same reducing capacity as Red in these systems: 2.9 μM. That is, 2.9 μM ascorbate would generate the same amount of reduction as 10^{11} cells l^{-1}.

Although reduction by ascorbate is much faster than microbially mediated reduction in these laboratory studies, the experimental conditions are not likely to be representative of the environment. The concentration of abiotic reductants may be substantially lower than the ascorbate concentration used. And conversely, the cell number (10^{11} cells l^{-1}) is at the low end of the environmental range in shallow sediments of 10^{11}–10^{13} cells l^{-1} (Capone and Kiene 1988, Wellsbury et al. 1996), although metal-reducing bacteria may be only a fraction of the total biomass.

Limitations of HMO-doped gel probes

Besides the above caveat regarding microbial reduction, HMO-doped gel probes are subject to three additional considerations. First, Mn readily leaches out of the HMO-doped gels at low rates in deionized water. This method of HMO synthesis uses excess Mn(II), which results in "pre-saturated" HMO sorption sites for laboratory experiments. On one hand, saturated sorption sites could avoid the issue of reduced Mn from the solid sorbing onto the surface, making bulk solution measurements of dissolved Mn(II) more representative of the surface reduction rate. On the other hand, Mn(II) could block access of reductants to the surface of HMO, depressing the measured rates. Nevertheless, since rates of HMO reduction are comparable to those in literature for both abiotic and microbially mediated reduction, this concern is minimal. In practice, desorption rates of Mn(II) are insignificant relative to reductive dissolution rates over the course of the laboratory experiments, but non-negligible amounts of Mn may be lost to low-ionic strength storage solution prior to the start of experiments, or in transport to the field. Storage in solutions with equivalent ionic strength to the field conditions and reduction of

the storage time will minimize this effect, but failure to account for this could lead to an overestimation of the amount of Mn loss via reduction.

Second, *S. oneidensis* MR-1 exhibited an 8 h lag phase in experiments with HMO-doped gels in mini-probes. A possible consequence for field application is that microbial metabolism could require some amount of time to adjust to the newly available oxidant. For this reason, deployment times should allow for the lag time ($\leq$ 8 h) to become insignificant relative to the total deployment time.

Finally, any field application of these gel probes must consider the impact of Mn addition to sediments. In sediments with high organic carbon sediments and high microbial activity but low Mn content, Mn-reducing physiology may be prevalent (Lovley 1991) but not active under ambient conditions. The introduction of HMO-doped gels would then introduce a substrate that was not present in the sediments and the measured rate of reduction based on the HMO-doped gels would represent a potential rate of reduction (rather than the actual rate under ambient conditions). To account for this, solid phase analysis of sediment cores should accompany deployment to show definitively where Mn oxide is exhausted in the sediment. In light of this consideration, this technique may be taken to represent a lower bound (i.e., corresponding to the indirect reduction pathway only) of the potential for Mn reduction (i.e., where the solid substrate is not limiting) in a saturated environment.

Acknowledgements

We would like to thank Dianne Newman, Doug Lies, Tracy Teal, and Alexa Price-Whelan for help in the selection, cultivation, and fluorescence microscopy of *S.*

oneidensis MR-1. Peter Reichert's assistance in working with AQUASIM is also appreciated. We gratefully acknowledge funding from an NSF Graduate Research Fellowship and NSF EAR-0525387, as well as from Eawag.